2026 8th Global Power, Energy and Communication Conference (GPECOM) | 979-8-3315-5204-6/26/$31.00 ©2026 IEEE | DOI: 10.1109/GPECOM70462.2026.11578656

Progressive Hedging Augmentations for Stochastic Frequency-Constrained Unit Commitment

Azeez O. Olasoji
Department of Electrical Engineering
University of Cape Town
Cape Town, South Africa
olsaze001@myuct.ac.za

David T.O. Oyedokun
Department of Electrical Engineering
University of Cape Town
Cape Town, South Africa
david.oyedokun@uct.ac.za

Juan Esteban Sierra-Aguillar
Department of Electrical Engineering
Universidad de Antioquia
Medellin, Colombia
juane.sierra@udea.edu.co

Mohammad Rajabdorri
IIT, ETSI-ICAI
Universidad Pontificia Comillas
Madrid, Spain
mrajabdorri@comillas.edu

Mkhutazi Mditshwa
Department of Electrical Engineering
University of Cape Town
Cape Town, South Africa
mdtmkh001@myuct.ac.za

Chukwuemeka E. Okafor
Department of Electrical Engineering
University of Cape Town
Cape Town, South Africa
okfchu002@myuct.ac.za

Komla A. Folly
Department of Electrical Engineering
University of Cape Town
Cape Town, South Africa
komla.folly@uct.ac.za

***Abstract*—This paper develops a two-stage stochastic frequency-constrained unit commitment (FCUC) model for low-inertia grids with wind-based synthetic inertia (SI) and solves it using Progressive Hedging (PH). Frequency-security limits on RoCoF, nadir and steady-state deviation are embedded through separable-programming linearisations. In the model, SI is not a free always-available input: its realised contribution is capped at 20% of wind-plant nameplate and linked to curtailment-gated SI power variables. The formulation is tested on the IEEE RTS-96 system under a high-wind, high-demand case with exogenous wind scenarios. Deterministic FCUC restores frequency security relative to conventional UC, while increasing SI from 0 s to 6 s reduces operating cost without losing non-negative frequency margins. For the stochastic FCUC, the extensive-form MILP is compared with two PH variants whose scenario subproblems become MIQPs because of quadratic proximal penalties on commitment variables. PH preserves the extensive-form frequency behaviour and cuts wall-clock time from 4451 s to 594–611 s, while keeping expected RoCoF and nadir margins non-negative.**

***Index Terms*—Frequency-constrained unit commitment (FCUC), synthetic inertia (SI), wind power integration, low-inertia power systems, mixed-integer linear programming (MILP), mixed-integer quadratic programming (MIQP), stochastic optimisation, progressive hedging (PH)**

I. Introduction

Power systems with growing shares of converter-interfaced generation are increasingly operated under low-inertia conditions. In such environments, credible contingencies can trigger large frequency excursions, and traditional unit commitment (UC) formulations that enforce only power balance and reserve requirements are no longer sufficient. Operators must ensure that committed units collectively provide enough inertia and primary frequency response (PFR) to satisfy limits on rate of change of frequency (RoCoF), frequency nadir, and steady-state deviation, in addition to meeting demand at minimum cost [1]. This has motivated a class of frequency-constrained unit commitment (FCUC) models, which embed analytical surrogates of frequency dynamics directly into the UC problem.

Most existing FCUC formulations are deterministic: they assume perfectly known demand and renewable production and optimise a single "typical" day or critical operating condition [1], [2]. While such models clarify the interaction between inertia, PFR headroom, and credible losses, they do not capture the variability and forecast uncertainty of wind generation. In low-inertia systems with substantial wind penetration, ignoring this uncertainty can lead to overly conservative schedules, with unnecessary commitment and reserve, or to schedules that appear secure in expectation but violate frequency limits under plausible wind realisations. However, enforcing explicit RoCoF, nadir and QSS limits using separable-programming approximations introduces additional binary and continuous variables, turning the UC into a large mixed-integer problem that is difficult to solve efficiently on large power system networks

Stochastic unit commitment (SUC) provides a principled way to hedge against renewable uncertainty by co-optimising first-stage commitment decisions and second-stage scenario-dependent dispatch [1]. However, most SUC studies enforce security through conventional reserve requirements and network constraints only; explicit frequency-security constraints and the contribution of synthetic inertia (SI) from wind plants are usually treated in separate dynamic studies or as ex-post checks. Moreover, solving a two-stage SUC with detailed DC power flow and frequency surrogates directly as a single extensive-form MILP becomes computationally challenging. The contribution of this paper is therefore not wind-scenario synthesis or controller-level transient validation, but tractable FCUC scheduling under exogenous wind uncertainty.

Progressive Hedging (PH) is a well-established primal decomposition method for scenario-based stochastic programs [3]. By iteratively coordinating scenario subproblems via consensus variables and penalty terms, PH can exploit parallelism and reduce the wall-clock time of solving large two-stage mixed-integer programs. Recent work has adapted PH to security-constrained UC with network constraints [4]; however, to the best of the authors' knowledge, there is limited study on the viability of PH for stochastic FCUC models that (i) enforce RoCoF, nadir and QSS limits via separable-programming approximations and (ii) explicitly represent wind-based SI capability within stochastic FCUC alongside commitment decisions.

This paper addresses these gaps by developing and evaluating a stochastic FCUC formulation with synthetic inertia on a 96-bus transmission test system. The model is two-stage: first-stage binary variables determine unit commitment and start-up decisions, while second-stage variables describe scenario-dependent dispatch, wind curtailment, DC power flows and frequency-related auxiliary variables for each wind-power scenario. Frequency security is enforced through analytical surrogates for RoCoF, nadir and QSS limits, reformulated via a change of variables and piecewise-linear SOS2 approximations. Synthetic inertia from wind farms is modelled as an additional post-fault inertia contribution proportional to a fixed emulated inertia setting at the converter level. The test system is based on the IEEE RTS-96 network with wind integration from [5].

To solve this problem, we implement a PH-augmented solution framework with DC power flow and separable-programming frequency constraints. Two PH variants are considered: a Watson–Woodruff-style scheme with fixed penalties and an Ordoudis-inspired variant with objective-scaled penalties and consensus projection. Both treat the underlying FCUC as a two-stage MILP, but the PH-augmented subproblems become MIQPs due to the quadratic proximal terms.

The main contributions are threefold: (i) a two-stage stochastic FCUC for IEEE RTS–96 with DC power flow, SP-based RoCoF/nadir/QSS constraints, and wind-based SI; (ii) two PH augmentation variants with cost–range and objective-scaled penalties; and (iii) a case study that compares economics, runtimes and frequency-security indicators across deterministic, extensive-form and PH-based formulations.

II. Unit Commitment Formulation and Frequency Constraints

This section outlines the frequency-constrained unit commitment (FCUC) model used in this work. The formulation is kept test-system agnostic; its instantiation on the IEEE 96-bus network with wind integration is described in Section IV. Sets, indices and symbols follow the Nomenclature.

A. Unit Commitment Formulation

We consider a standard thermal unit commitment model with DC power flow and curtailable wind generation. For each time period $t \in \mathcal{T}$, generator $i \in \mathcal{G}$, bus $s \in \mathcal{B}$, line $\ell \in \mathcal{L}$, and wind unit $w \in \mathcal{W}$, the main decision variables are:

- $x_{t,i} \in \{0,1\}$: on/off status of generator i,
- $y_{t,i}, z_{t,i} \in \{0,1\}$: start-up and shutdown indicators,
- $g_{t,i} \geq 0$: total active power output,
- $g^{\text{lin}}_{t,i,b} \geq 0$: block outputs for piecewise-linear fuel cost,
- $\theta_{t,s}$: bus voltage angles (slack bus fixed),
- $p_{t,\ell}$: active power flows on lines,
- $\text{curt}_{t,w} \geq 0$: curtailed wind power.

Let $C^{\text{fuel}}_t(x_t, g_t)$ denote the fuel cost (fixed plus linear block cost) and $C^{\text{su}}_t(y_t)$ the start-up cost; wind curtailment is penalised by ω^{curt}. The UC objective is shown below

$$\min \sum_{t\in\mathcal{T}} \Big[C^{\text{fuel}}_t(x_t, g_t) + C^{\text{su}}_t(y_t) + \omega^{\text{curt}} \sum_{w\in\mathcal{W}} \text{curt}_{t,w} \Big]. \quad (1)$$

The objective is constrained by standard UC constraints, depicted below:

$$\text{Power balance:} \quad \sum_{i\in\mathcal{G}_s} g_{t,i} + \sum_{w\in\mathcal{W}_s} \big(P^{\text{wind}}_{t,w} - \text{curt}_{t,w}\big) - \sum_{\ell\in\mathcal{L}} a_{\ell s} p_{t,\ell} = D_{t,s}, \quad (2a)$$

$$\text{DC power flow:} \quad p_{t,\ell} = B_\ell \sum_{s\in\mathcal{B}} a_{\ell s}\theta_{t,s}, \quad (2b)$$

$$\text{Line limits:} \quad -F^{\max}_\ell \leq p_{t,\ell} \leq F^{\max}_\ell, \quad (2c)$$

$$\text{Unit limits:} \quad P^{\min}_i x_{t,i} \leq g_{t,i} \leq P^{\max}_i x_{t,i}, \quad (2d)$$

$$\text{Piecewise fuel cost:} \quad g_{t,i} = \sum_b g^{\text{lin}}_{t,i,b}, \quad 0 \leq g^{\text{lin}}_{t,i,b} \leq \bar{P}_{i,b} x_{t,i}. \quad (2e)$$

Logic, minimum up/down times and ramp constraints on $(x_{t,i}, y_{t,i}, z_{t,i})$ follow standard UC formulations.

The two-stage stochastic UC formulation (Section III) is built on this base model by replicating the dispatch, network and frequency-related variables per scenario, while keeping the commitment variables $x_{t,i}$ and start-up/shutdown decisions first-stage.

B. Frequency-Security Constraints via Separable Programming

Frequency security is enforced through analytical surrogates for RoCoF, nadir and quasi steady-state (QSS) limits. Let $H_{\text{sys}}(t)$ and $R_{\text{sys}}(t)$ denote the aggregate inertia and primary frequency response (PFR) headroom at time t, and let $\Delta P(t)$ denote the largest credible infeed loss, see [2] for more details.

The pre-fault totals are

$$H_{\text{sys}}(t) = \sum_{i\in\mathcal{G}} H_i M_i x_{t,i} + H^{\text{SI}}_{\text{wind}}(t), \quad (3)$$

$$R_{\text{sys}}(t) = \sum_{i\in\mathcal{G}} \big(P^{\max}_i x_{t,i} - g_{t,i}\big), \quad (4)$$

where H_i and M_i are the inertia constant and MVA base of each unit, and $H^{\mathrm{SI}}_{\mathrm{wind}}(t)$ is the synthetic inertia contribution from wind (Section II-C). The credible loss $\Delta P(t)$ is represented via an SOS2 interpolation on a grid $\{\Delta P^p\}$ up to $\Delta P_{\max}$.

Similar to [2], we introduce a change of variables

$$x_1(t) = \tfrac{1}{2}\big(\alpha H_{\mathrm{sys}}(t)+\beta R_{\mathrm{sys}}(t)\big), \quad x_2(t) = \tfrac{1}{2}\big(\alpha H_{\mathrm{sys}}(t)-\beta R_{\mathrm{sys}}(t)\big), \tag{5}$$

with positive constants α, β. The pair $\big(x_1(t), x_1^2(t)\big)$ and $\big(x_2(t), x_2^2(t)\big)$ is obtained via SOS2-based piecewise-linear interpolation, so that the resulting frequency constraints remain linear in the auxiliary variables.

Using these transformed variables, the RoCoF, QSS and nadir inequalities take the form

$$\text{RoCoF:} \quad \frac{x_1(t)+x_2(t)}{\alpha} \;\geq\; \frac{f_0}{2\,\mathrm{RoCoF}_{\max}}\,\Delta P(t), \tag{6}$$

$$\text{QSS:} \quad \frac{x_1(t)-x_2(t)}{\beta} \;\geq\; \Delta P(t) - D_{\mathrm{load}} P_D(t)\,\Delta f_{\mathrm{ss}}, \tag{7}$$

$$\text{Nadir (SP):} \quad x_1^2(t) - x_2^2(t) \;\geq\; \alpha\beta\bigg(\frac{f_0 T_g}{4\Delta f_{\max}}\,\Delta P^2(t) - \frac{D_{\mathrm{load}} P_D(t) T_g f_0}{4}\,\Delta P(t)\bigg), \tag{8}$$

where f_0 is the nominal frequency, $P_D(t) = \sum_s D_{t,s}$ is the total demand, T_g is an effective governor time constant, and $\Delta f_{\max}$, Δf_{ss} and $\mathrm{RoCoF}_{\max}$ are the admissible nadir, steady-state deviation and RoCoF limits, respectively. Also, a fixed load-damping coefficient is assumed throughout the study. This term represents the aggregate frequency sensitivity of demand and is introduced to retain a tractable analytical FCUC formulation. Hence, D_{load} is treated as a modelling parameter rather than a decision variable. All nonlinear terms in (8) and in the definition of $\Delta P^2(t)$ are handled via SOS2 approximations.

C. Synthetic Inertia from Wind

Synthetic inertia (SI) from wind plants is represented through a fixed converter-emulation constant H_{wind}, while the effective SI power contribution is optimisation-dependent. In the implemented model, SI is not an unconstrained abstract knob. Instead, each wind unit $w \in \mathcal{W}$ is assigned SI power variables that are capped at a fixed fraction of nameplate capacity and split into curtailment-supported and non-curtailed components, namely

$$p^{\mathrm{SI}}_{t,w} \leq \phi^{\mathrm{SI}}\,\bar{P}^W_w, \tag{9a}$$

$$p^{\mathrm{SI}}_{t,w} = p^{\mathrm{SI,curt}}_{t,w} + p^{\mathrm{SI,wind}}_{t,w}, \tag{9b}$$

$$p^{\mathrm{SI,curt}}_{t,w} \leq \mathrm{curt}_{t,w}, \tag{9c}$$

$$p^{\mathrm{SI,wind}}_{t,w} \leq \big(1 - y^{\mathrm{curt}}_{t,w}\big)\phi^{\mathrm{SI}}\,\bar{P}^W_w, \tag{9d}$$

where $\phi^{\mathrm{SI}} = 0.2$ is the SI nameplate cap fraction and the binary indicator $y^{\mathrm{curt}}_{t,w}$ activates the curtailment-gated logic used to prevent double counting of curtailed and non-curtailed wind contributions. In the stochastic extensive form and in each PH scenario subproblem, the same SI logic is applied per scenario.

TABLE I
KEY FREQUENCY-SECURITY AND SYNTHETIC INERTIA PARAMETERS.

Parameter	Symbol	Value
Nominal frequency	f_0	50 Hz
RoCoF limit	$\mathrm{RoCoF}_{\max}$	0.5 Hz/s
Nadir limit	$\Delta f_{\max}$	0.8 Hz
Steady-state deviation limit	Δf_{ss}	0.5 Hz
Load damping factor	D_{load}	0.01 pu
Governor time constant	T_g	10 s
Max credible loss	$\Delta P_{\max}$	400 MW
SI power cap fraction	ϕ^{SI}	0.2
Wind emulated inertia	H_{wind}	6 s

The effective inertia in (3) is therefore written as

$$H_{\mathrm{sys}}(t) = \sum_{i\in\mathcal{G}} H_i M_i x_{t,i} - H^\star M^\star + \sum_{w\in\mathcal{W}} H_{\mathrm{wind}}\,p^{\mathrm{SI}}_{t,w}, \tag{10}$$

where $H^\star M^\star$ represents the contribution of the largest infeed lost in the contingency. In this study, H_{wind} is an exogenous converter setting: the deterministic FCUC benchmark is used to examine the sensitivity of operating cost and frequency margins to varying SI levels, while the stochastic and PH-augmented formulations focus on a practically motivated non-zero setting. No standalone SI remuneration term is included; its economic effect enters indirectly through commitment, reserve and curtailment decisions.

This representation is intentionally at the scheduling layer. It captures how wind-based SI changes commitment, reserve headroom and operating cost, but it does not explicitly model converter activation delay, rotor-speed recovery, saturation effects, or EMT-level transients. Hence, this study focuses solely on FCUC (at a planning level-day ahead) study rather than a controller-design or time-domain validation study. We take $\Delta P_{\max} = 400$ MW as the credible loss of the largest conventional unit. Basic frequency and SI-related parameters are summarised in Table I.

III. Stochastic FCUC and Progressive Hedging

A. Two-Stage Stochastic FCUC (MILP Extensive Form)

We model wind uncertainty via a finite exogenous scenario set Ω with probabilities p_ω, $\sum_\omega p_\omega = 1$. The first-stage variables are only the scenario-independent commitment and start-up/shut-down decisions $x_{t,i}$, $y_{t,i}$ and $z_{t,i}$. For each scenario $\omega \in \Omega$, the second-stage variables include generator dispatch $g_{t,i,\omega}$, block outputs $g^{\mathrm{lin}}_{t,i,b,\omega}$, wind curtailment $\mathrm{curt}_{t,w,\omega}$, line flows $f_{t,\ell,\omega}$, bus angles $\theta_{t,s,\omega}$, the scenario-dependent split of synthetic-inertia power, and the auxiliary variables associated with the separable-programming (SP) frequency constraints.

In compact form, the two-stage stochastic FCUC problem reads

$$\min_{x,y,z,\{g_\omega,\dots\}} \sum_{\omega\in\Omega} p_\omega \sum_{t\in\mathcal{T}} C_t\big(x,y,z,g_{t,\omega},\mathrm{curt}_{t,\omega},\dots\big) \tag{11}$$

$$\text{s.t.} \quad (x,y,z) \in \mathcal{X}, \tag{12}$$

$$(g_\omega, \mathrm{curt}_\omega, f_\omega, \theta_\omega, \dots) \in \mathcal{Y}_\omega(x) \quad \forall \omega \in \Omega, \tag{13}$$

where $\mathcal{X}$ collects the standard UC constraints (minimum up/down times, ramping, startup-cost logic) and $\mathcal{Y}_\omega(x)$ contains, for each scenario, the DC power-balance and line-flow constraints plus the SP-based RoCoF, nadir and QSS inequalities introduced in Section II. Because all SP frequency constraints are expressed as linear inequalities in x_1, x_2, x_1^2, x_2^2, ΔP and ΔP^2, the extensive-form model (11)–(13) is a *mixed-integer linear program (MILP).* [1]

B. Progressive Hedging Augmentation (MILP Base, MIQP Subproblems)

To improve tractability for larger scenario sets, we apply Progressive Hedging (PH) to the two-stage FCUC in (11)–(13), treating the commitment variables $x_{t,i}$ as first-stage consensus variables. The underlying stochastic FCUC is a MILP; PH augments each scenario $\omega \in \Omega$ with linear and quadratic penalty terms on $x_{t,i,\omega}$, so that the resulting per-scenario problems become mixed-integer quadratic programs (MIQPs).

At PH iteration k, each scenario subproblem is solved independently with augmented objective

$$\sum_t C_t(\cdot) + \sum_{t,i} \Big(W^{(k)}_{t,i,\omega} x^{(k)}_{t,i,\omega} + \tfrac{1}{2}\rho^{(k)}_{t,i} (x^{(k)}_{t,i,\omega} - \hat{x}^{(k)}_{t,i})^2 \Big), \quad (14)$$

subject to the UC, DC power-flow and SP frequency constraints for scenario ω. The quadratic term acts only on the binary $x^{(k)}_{t,i,\omega}$, so if it is removed (e.g., in a final evaluation solve) the subproblems revert to MILPs.

After solving all scenarios, PH forms a probability-weighted consensus

$$\tilde{x}^{(k)}_{t,i} = \sum_{\omega \in \Omega} p_\omega x^{(k)}_{t,i,\omega}, \qquad \hat{x}^{(k)}_{t,i} = \Pi_{\{0,1\}}\big(\tilde{x}^{(k)}_{t,i}\big), \quad (15)$$

where $\Pi_{\{0,1\}}(\cdot)$ denotes component-wise projection onto $\{0,1\}$. Scenario multipliers are then updated as

$$W^{(k+1)}_{t,i,\omega} = W^{(k)}_{t,i,\omega} + \rho^{(k)}_{t,i} \big(x^{(k)}_{t,i,\omega} - \hat{x}^{(k)}_{t,i} \big), \quad (16)$$

and the process is repeated until consensus metrics and a probability-weighted mean MIP gap satisfy prescribed tolerances. Algorithm 1 summarises the iteration.

Because the first-stage variables are binary, PH is used here as a decomposition heuristic for the mixed-integer stochastic FCUC rather than as an exact globally convergent method. In the present implementation, PH penalises only the commitment variables $\{x_{t,i,\omega}\}$; start-up category variables are not assigned separate proximal penalties. Two penalty-design variants are compared. For the Watson–Woodruff-style variant, the penalty update applied after the first PH iteration is

$$\rho^{\mathrm{WW}}_{t,i} = 10 \, \frac{a_i}{x^{\max}_{t,i} - x^{\min}_{t,i} + 1}, \quad (17)$$

[1] In practice we solve the deterministic FCUC and the extensive form with a MILP/QP-capable solver; however, without PH penalties the mathematical structure is linear in the decision variables.

Algorithm 1 Progressive Hedging for Stochastic FCUC

Require: Scenario set Ω, probabilities p_ω, PH tolerances, minimum iterations $K_{\min}$
Initialise $k \leftarrow 1$, $W^{(1)}_{t,i,\omega} \leftarrow 0$, choose initial $\rho^{(1)}_{t,i}$
repeat
  for all $\omega \in \Omega$ **do**
    Solve scenario FCUC MIQP for ω with objective (14) and UC + DC PF + SP constraints
  end for
  Compute $\tilde{x}^{(k)}_{t,i} = \sum_\omega p_\omega x^{(k)}_{t,i,\omega}$
  Project to binary consensus $\hat{x}^{(k)}_{t,i} = \Pi_{\{0,1\}}(\tilde{x}^{(k)}_{t,i})$
  for all t, i, ω **do**
    Update multipliers using (16)
  end for
  Optionally update $\rho^{(k+1)}_{t,i}$ (Watson–Woodruff or Ordoudis-type scaling)
  Compute consensus norms and mean MIP gap; set $k \leftarrow k + 1$
until $k \geq K_{\min}$ and all stopping tolerances are met

where $x^{\max}_{t,i}$ and $x^{\min}_{t,i}$ are the first-iteration scenario-wise maxima and minima of $x_{t,i,\omega}$. For the objective-scaled variant, we define a cost share $h_i = a_i / (\sum_j |a_j| + \varepsilon)$ and use

$$\rho^{\mathrm{Ord}}_{t,i} = \mathrm{clip}(\bar{z}\, h_i, 10^{-6}, 10^{6}), \quad (18)$$

where $\bar{z} = \sum_{\omega \in \Omega} p_\omega z^{(1)}_\omega$ is the probability-weighted first-iteration scenario objective. After PH terminates, the projected binary consensus is fixed and each scenario is re-solved without PH quadratics in a consensus-polishing step; the reported PH economics and frequency metrics correspond to this polished consensus evaluation. In both variants the base two-stage model remains a MILP; PH introduces MIQP subproblems only through the quadratic proximal terms on $x_{t,i,\omega}$.

IV. Case Study and Simulation Setup

A. System Data and Wind Uncertainty

The deterministic and stochastic FCUC formulations are evaluated on a modified IEEE RTS–96 system [5] with 96 buses, 120 lines, 96 thermal units and 19 wind plants over a 24 h horizon. The load profile corresponds to a high-demand day, and the largest in-feed is a 400 MW nuclear unit, which defines the $N{-}1$ credible contingency in the frequency constraints.

Wind generation is represented by bus-located plants whose aggregate annual energy share corresponds to 50% penetration. In the deterministic FCUC, wind follows a single "median" day-ahead trajectory. In the stochastic FCUC, wind uncertainty is represented by a finite exogenous scenario set Ω with probabilities p_ω, scaled so that each scenario preserves the 50% penetration target over 24 h. These wind scenarios are treated as stochastic inputs, in the spirit of scenario-based low-inertia SUC studies [6], rather than being generated within the present paper.

The study system is treated as a self-secured balancing area; external emergency support from neighbouring areas, HVDC links, or inter-area primary frequency response is not modelled.

SI is supplied by the wind plants via a fixed converter setting $H_{\text{wind}} = 6$ s for all stochastic FCUC cases. Deterministic

TABLE II
SUMMARY OF SIMULATION CASES.

Case ID	Model type	PH variant	H_{wind} [s]	# scen.
D–MILP	Deterministic FCUC (MILP)	–	0–6	–
S–Ext	Stochastic FCUC (extensive form, MILP)	–	6	$\lvert\Omega\rvert$
S–PH–WW	Stochastic FCUC + PH (MIQP)	Watson–Woodruff	6	$\lvert\Omega\rvert$
S–PH–Ord	Stochastic FCUC + PH (MIQP)	Ordoudis–scaled	6	$\lvert\Omega\rvert$

sensitivity runs with $H_{\text{wind}} \in \{0, \ldots, 6\}$ s are used only to contextualise the stochastic results; for comparison in this paper we report the deterministic FCUC case with $H_{\text{wind}} = 6$ s.

B. Simulation Cases and PH Settings

We study four cases on the same IEEE RTS–96 network, wind scenarios, and frequency parameters. SI sensitivity is examined only in the deterministic study ($H_{\text{wind}} \in [0, 6]$ s), whereas all stochastic results use $H_{\text{wind}} = 6$ s. The deterministic and extensive stochastic FCUC models are MILPs; PH scenario subproblems are MIQPs due to the quadratic proximal terms. The cases are summarised in Table II.

In PH, each iteration solves independent scenario subproblems with scenario-specific commitments $x_{t,i,\omega}$ and multipliers $W_{t,i,\omega}$. The consensus commitment is the probability-weighted mean $\hat{x}_{t,i} = \sum_{\omega\in\Omega} p_\omega x_{t,i,\omega}$, which is projected to binaries using $\alpha_{\text{PH}} = 0.55$ and $\beta_{\text{PH}} = 0$. Scenario agreement is monitored by two consensus residuals: $gg = \sum_{t,\omega,i} p_\omega |x_{t,i,\omega} - \hat{x}_{t,i}|$ and $td = |\Omega|^{-1}\sum_{t,\omega,i:\hat{x}_{t,i}>0} |x_{t,i,\omega} - \hat{x}_{t,i}|/\hat{x}_{t,i}$, representing, respectively, the probability-weighted absolute and normalized disagreement from consensus. Smaller gg and td therefore indicate tighter alignment of scenario commitments. After a minimum of five PH iterations, the algorithm stops if any of $gg \leq 10^{-5}$, $td \leq 10^{-5}$, or $GapMean_{\text{iter}} \leq 10^{-2}$ is satisfied; otherwise, it is capped at 10 iterations. The Watson–Woodruff and objective-scaled penalties follow (17) and (18), respectively.

C. Implementation and Performance Metrics

All models are implemented in GAMS and solved with CPLEX. The deterministic and extensive-form stochastic FCUC instances are treated as MILPs. In the PH-augmented cases, the quadratic proximal terms on the commitment variables turn each scenario subproblem into an MIQP, while the final evaluation runs (without proximal terms) revert to MILPs. Unless stated otherwise, we use a 1% relative MIP gap and, for stochastic cases, a 24 h wall-clock limit. All simulations are carried out on a laptop with an Intel Core i7 processor (2.8 GHz) and 16 GB of RAM.

We report three groups of indicators: (i) economic (total or expected operating cost and startup cost); (ii) computational (solver runtime, final MIP gap and, for PH, the number of iterations and consensus metrics at termination); and (iii) frequency-security (minimum expected RoCoF and nadir margins and the maximum nadir violation probability over the horizon). These quantities underpin the comparisons in Section V.

V. RESULTS AND DISCUSSION

A. Computational Performance and Economic Outcomes

Table III reports economic, computational and frequency-security indicators for the deterministic ($H_{\text{wind}} = 0 - 6$ s) and stochastic FCUC formulations at $H_{\text{wind}} = 6$ s. For deterministic runs, C^{tot} is the 24-hour operating cost; for stochastic runs it is the expected cost $\mathbb{E}[C^{\text{tot}}]$. "Optimality gap" is the final MIP gap (for PH, the max. gap across scenarios is shown in parentheses), and runtimes are wall-clock times. Curtailment energy is zero in all cases for the high-wind, high-demand simulation conducted.

The deterministic noFCUC case is cheapest (\$1.022 million) and fastest (49 s), but yields very low inertia ($H_{\min} = 8{,}470$ MW s), large negative RoCoF and nadir margins, and 100% nadir violation probability; it serves as an economic lower bound but is clearly infeasible from a frequency-security perspective. Enforcing the FCUC constraints with $H_{\text{wind}} = 0$ s raises the cost to \$1.092 million, but yields a frequency-secure schedule: the expected RoCoF and nadir margins become (slightly) positive and the nadir violation probability drops from 100% to 0%. As H_{wind} is raised from 0 s to 6 s, the total cost decreases monotonically to \$1.072 million, while average inertia rises and the required PFR headroom R_{mean} drops, showing that synthetic inertia partly substitutes for conventional reserves without sacrificing frequency margins.

The stochastic formulations further reduce expected cost while keeping frequency margins tight. The extensive-form SUC achieves \$1.048 million with a small gap (0.38%) but requires a long runtime (4,451 s). The PH variants reduce this wall-clock time to 594 s and 611 s, corresponding to speed-up factors of approximately 7.5 and 7.3, respectively, while preserving the same FCUC physics. PH–WW and PH–Ord return final gaps of 0.05% and 0.1%, and expected costs of \$1.058 million and \$1.046 million, respectively. In all stochastic cases, the minimum expected RoCoF and nadir margins remain essentially binding yet non-negative. The worst-hour nadir violation probabilities ($\max_t P^{\text{nadir}}_{\text{viol}}(t)$) lie between 14.7% and 25.1%, indicating that only a limited fraction of scenarios at a few critical hours exceed the nadir limit, a trade-off that could be tightened further via explicit risk constraints or stricter PH penalty settings.

B. Frequency-Security Profiles

Figures 1 and 2 show the hourly RoCoF and nadir profiles for the deterministic UC without frequency constraints and for all FCUC formulations at $H_{\text{wind}} = 6$ s. For the stochastic cases, the curves represent expected values across wind scenarios; for the deterministic runs they coincide with the single trajectory.

The baseline UC without FCUC constraints violates both limits by a wide margin in several hours, with RoCoF and nadir excursions well above the prescribed thresholds. Imposing FCUC constraints and $H_{\text{wind}} = 6$ s keeps all deterministic and stochastic trajectories below the RoCoF and nadir limits over the entire day. The most critical hours correspond to the HWHD periods highlighted in the plots, where load is high

TABLE III
ECONOMIC, COMPUTATIONAL, AND FREQUENCY-SECURITY INDICATORS FOR DETERMINISTIC AND STOCHASTIC FCUC FORMULATIONS.

Case	C^{tot} [\$]	Optimality gap [%]	Runtime [s]	Curtailment Energy [MWh]	$H_{\min}$ [MW·s]	H_{avg} [MW·s]	R_{mean} [MW]	$\min_t \mathbb{E}$[RoCoF marg.] [Hz/s]	$\min_t \mathbb{E}$[nadir marg.] [Hz]	$\max_t P^{\text{nadir}}_{\text{viol}}(t)$ [%]
Deterministic noFCUC	1,022,206	0.5	48.9	0	8,470	20,418	449	-0.68	-6.18	100
Deterministic FCUC, SI = 0 s	1,092,433	0.94	158.3	0	20,001	24,913	1,752	2.94e−5	2.51e−3	0
Deterministic FCUC, SI = 2 s	1,076,664	0.48	21.4	0	20,000	25,960	883	2.0e−2	2.7e−3	0
Deterministic FCUC, SI = 4 s	1,072,323	0.75	27.6	0	20,168	27,358	822	4.2e−3	1.1e−16	0
Deterministic FCUC, SI = 5 s	1,071,849	0.87	45.1	0	20,000	27,662	816	1.7e−2	9.7e−5	0
Deterministic FCUC, SI = 6 s	1,071,730	0.99	29.6	0	21,131	28,647	782	2.7e−2	0	0
Stochastic FCUC (ext. form)	1,047,972	0.38	4,451	0	20,000	26,841	741	1.6e−2	9.9e−5	14.7
PH Stochastic FCUC (WW)	1,057,952	0.05 (0.2)	594	0	20,000	28,775	902	1.6e−2	7.7e−16	25.1
PH Stochastic FCUC (Ord)	1,045,525	0.1 (0.44)	611	0	20,000	28,562	911	1.6e−2	4e−17	24.2

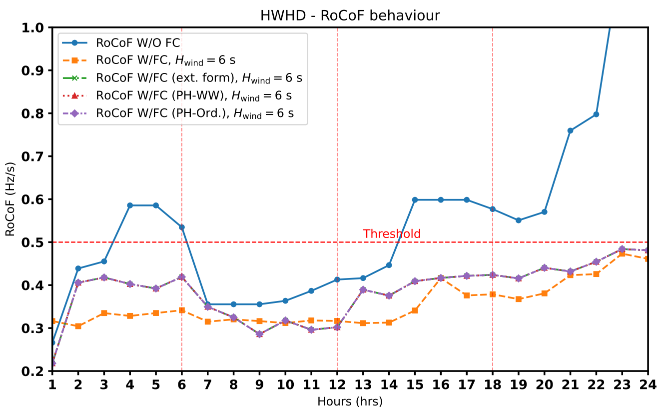

Fig. 1. RoCoF trajectories for the HWHD case; the horizontal line marks the RoCoF limit.

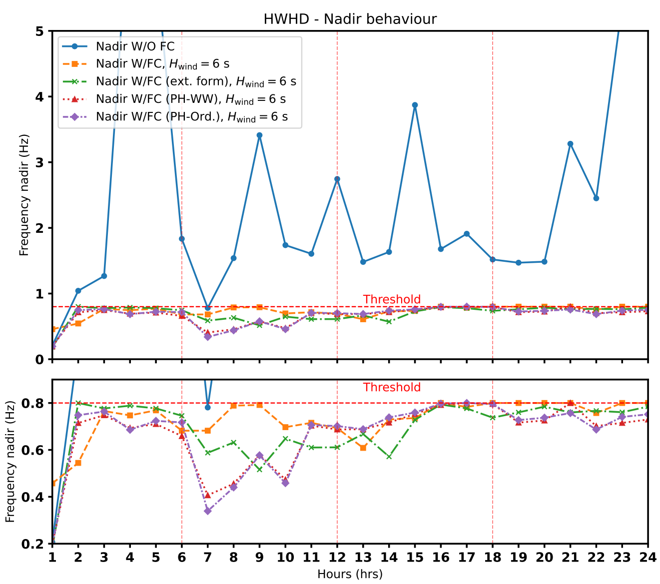

Fig. 2. Frequency nadir trajectories for the HWHD case; the lower panel zooms in on the hours closest to the nadir limit.

and the 400 MW outage is most stressing; in these windows the stochastic formulations allocate slightly more inertia and PFR headroom, leading to trajectories that sit a little further away from the limits than the deterministic FCUC case.

The three stochastic variants (extensive form, PH–WW and PH–Ord) produce very similar RoCoF and nadir profiles, with only small deviations in the most stressed hours, indicating that the PH augmentation preserves the underlying frequency behaviour of the extensive-form stochastic FCUC. The summary metrics in Table III (minimum expected margins and maximum nadir violation probabilities) are consistent with these plots: all FCUC+SI cases maintain non-negative expected margins, while the residual frequency risk in the stochastic runs remains confined to a small set of hours with moderate $P^{\text{nadir}}_{\text{viol}}(t)$.

VI. CONCLUSION

This paper presented a stochastic FCUC for IEEE RTS–96 with SP-based RoCoF, nadir and QSS constraints and curtailment-gated wind-based SI. Conventional UC is cheapest but frequency-insecure, whereas FCUC restores security; increasing SI from 0 s to 6 s then lowers cost while retaining non-negative margins. The extensive-form MILP provides the stochastic benchmark, while PH reduces runtime from 4451 s to 594–611 s with similar expected costs and frequency margins. The formulation remains a scheduling-layer approximation, with fixed load damping and no explicit external support, activation delay, rotor-speed recovery or detailed transient converter dynamics.

REFERENCES

[1] Azeez O. Olasoji, D.T.O. Oyedokun, Samuel O. Omogoye, and Chris Thron. Review of frequency response strategies in renewable-dominated power system grids: Market adaptations and unit commitment formulation. *Scientific African*, 26:1–21, 2024.

[2] Carlos J Ferrandon-Cervantes, Behzad Kazemtabrizi, and Matthias CM Troffaes. Inclusion of frequency stability constraints in unit commitment using separable programming. *Electric Power Systems Research*, 203:107669, 2022.

[3] Jean-Paul Watson and David L Woodruff. Progressive hedging innovations for a class of stochastic mixed-integer resource allocation problems. *Computational Management Science*, 8(4):355–370, 2011.

[4] Cristian Camilo Marín-Cano, Juan Esteban Sierra-Aguilar, Jesús M López-Lezama, Álvaro Jaramillo-Duque, and Juan G Villegas. A novel strategy to reduce computational burden of the stochastic security constrained unit commitment problem. *Energies*, 13(15):3777, 2020.

[5] Hrvoje Pandžić, Yury Dvorkin, Ting Qiu, Yishen Wang, and Daniel S Kirschen. Toward cost-efficient and reliable unit commitment under uncertainty. *IEEE Transactions on Power Systems*, 31(2):970–982, 2015.

[6] Matthieu Paturet, Uros Markovic, Stefanos Delikaraoglou, Evangelos Vrettos, Petros Aristidou, and Gabriela Hug. Stochastic unit commitment in low-inertia grids. *IEEE Transactions on Power Systems*, 35(5):3448–3458, 2020.